Theor. Comput. Fluid Dyn. (2012) 26:291–310
DOI 10.1007/s00162-011-0230-1

ORIGINAL ARTICLE

A.V. Kuznetsov

Nanofluid bioconvection: interaction of microorganisms oxytactic upswimming, nanoparticle distribution, and heating/cooling from below

Received: 4 September 2010 / Accepted: 8 March 2011 / Published online: 24 March 2011

Abstract The aim of this paper is to develop a theory describing the onset of convection instability (called here nanofluid bioconvecion) that is induced by simultaneous effects produced by oxytactic microorganisms, nanoparticles, and vertical temperature variation. The theory is developed for the situation when the nanofluid occupies a shallow horizontal layer of finite depth. The layer is defined as shallow as long as oxygen concentration at the bottom of the layer is above the minimum concentration required for the bacteria to be active (to actively swim up the oxygen gradient). The lower boundary of the layer is assumed rigid, while at the upper boundary both situations when the boundary is rigid or stress free are considered. Physical mechanisms responsible for the slip velocity between the nanoparticles and the base fluid, such as Brownian motion and thermophoresis, are accounted for in the model. A linear instability analysis is performed, and the resulting eigenvalue problem is solved analytically using the Galerkin method.

Keywords Nanofluid bioconvection · Oxytactic microorganisms · Brownian motion · Thermophoresis · Natural convection · Horizontal layer

1 Introduction

There is significant potential in applications of nanofluids in various types of microsystems. These include micro heat pipes [1], microchannel heat sinks [2], and microreactors [3]. There is also a strong interest in using nanomaterials in different bio-microsystems, such as enzyme biosensors [4]. Reference [5] simulated the performance of a bioseparation system for capturing nanoparticles. There is also interest in developing chip-size microdevices for evaluating nanoparticle toxicity; for example, [6] suggested a biomimetic microsystem that reconstitutes the critical functional alveolar–capillary interface of a human lung to evaluate toxic and inflammatory responses of the lung to silica nanoparticles. Bioconvection has potential applications in bio-microsystems due to mass transport enhancement and mixing, which are important issues in many microsystems [7,8]. Also, the results presented in [9] suggest using bioconvection in a toxic compound sensor due to the ability of some toxic compounds to inhibit the flagella movement and thus suppress bioconvection.

The purpose of this paper is proposing a novel type of a nanofluid that involves both nanoparticles and oxytactic microorganisms, such as a soil bacterium *Bacillus subtilis*. These bacteria are oxygen consumers, and they swim up the oxygen concentration gradient. If the upper surface of a fluid layer is open to the atmosphere, these bacteria generally swim toward the upper region, which leads to a higher concentration of these microorganisms in the top region of the fluid. Since these bacteria are about 10% denser than water, they are known

Communicated by: Knio.

A.V. Kuznetsov(✉)
Department of Mechanical and Aerospace Engineering, North Carolina State University, Campus Box 7910, Raleigh, NC 27695-7910, USA
E-mail: avkuznet@eos.ncsu.edu

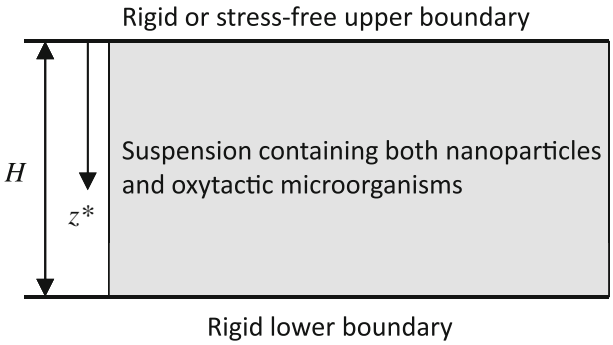

Fig. 1 Schematic diagram of the problem

to cause bioconvection, a phenomenon that occurs when convection instability is induced by upswimming microorganisms that are heavier than water [10–14].

For the presented research, the situation when convection is caused by a combined effect of oxytacic microorganisms and a vertical temperature variation is of particular interest. Such bio-thermal convection was considered in [15–18]. Bioconvection in nanofluids is anticipated to be possible if the concentration of nanoparticles is small, so that nanoparticles do not cause any significant increase in the viscosity of the base fluid. The problem of bioconvection in suspensions containing small solid particles (nanoparticles) was first considered in [19–23]. These papers addressed suspensions of gyrotactic microorganisms. The theory of such suspensions was further developed by Kuznetsov [24], who, utilizing Buongiorno's theory of convective transport in nanofluids [25] (this theory was applied to analyzing the onset of instability in nanofluids in [26,27]), included in the model physical mechanisms responsible for the slip velocity between the nanoparticles and the base fluid, such as Brownian motion and thermophoresis. The purpose of this paper is to extend the theory developed in [24] to the case of suspensions of oxytactic microorganisms. This is a more challenging task because the swimming velocity of oxytactic microorganisms is determined by the gradient of oxygen concentration; thus, in addition to all other phenomena, oxygen transport has to be modeled as well.

2 Governing equations

A water-based nanofluid containing nanoparticles and oxytactic microorganisms is considered. The nanofluid occupies a horizontal layer of depth H (Fig. 1). The nanoparticle suspension is assumed to be stable (there is no nanoparticle agglomeration). There are experimental techniques that make it possible to prepare nanoparticle suspensions that remain stable for several weeks [28]. The presence of nanoparticles is assumed to have no effect on the direction of microorganisms' swimming and on their swimming velocity. This is a reasonable assumption if the nanoparticle suspension is dilute (nanoparticle concentration is less than 1%). Bioconvection-induced flow is expected to occur only in a dilute suspension of nanoparticles; otherwise, a large concentration of nanoparticles would result in a large suspension viscosity, which would suppress bioconvection.

The governing equations are based on those presented in Buongiorno [25] and Nield and Kuznetsov [26,27]. The buoyancy term due to microorganisms' upswimming in the momentum Eq. (2) and conservation equation for microorganisms (6) are based on [10,11,15,16]. The governing equations are

$$\nabla \cdot \mathbf{U}^* = 0 \tag{1}$$

where $\mathbf{U}^* = (u^*, v^*, w^*)$ is the nanofluid velocity.

Introducing the buoyancy force and adopting the Boussinesq approximation, the momentum equation is written as

$$\rho_{f0}\left(\frac{\partial \mathbf{U}^*}{\partial t^*} + \mathbf{U}^* \cdot \nabla \mathbf{U}^*\right) = -\nabla^* p^* + \mu \nabla^{*2} \mathbf{U}^* + \left[\phi^* \rho_p + \left(1-\phi^*\right)\left\{\rho_{f0}\left(1-\beta\left(T^*-T_c^*\right)\right)\right\} + n^* \theta \Delta\rho\right]\mathbf{g} \tag{2}$$

where T^* is the nanofluid temperature, T_c^* is the reference temperature (the temperature of the upper wall), p^* is the pressure, n^* is the concentration of microorganisms, ϕ^* is the nanoparticle concentration, t^* is the

time, ρ_{f0} is the base-fluid density at the reference temperature, ρ_p is the density of the nanoparticles' material, β is the volumetric coefficient of thermal expansion of the base fluid, θ is the average volume of a microorganism, $\Delta\rho = \rho_{\mathrm{mo}} - \rho_{f0}$ is the density difference between a microorganism and a base fluid, $\mathbf{g}$ is the gravity vector, and μ is the viscosity of the suspension (the suspension contains the base fluid, nanoparticles, and microorganisms; μ is assumed to be constant). Asterisks denote dimensional variables. The approximation in Eq. (2) is valid when ϕ^* is small.

The Boussinesq approximation is extended to linearize the right-hand side of Eq. (2) by neglecting the term $\phi^*\rho_{f0}\beta\left(T^* - T_c^*\right)\mathbf{g}$. This assumption is expected to hold for a dilute suspension of nanoparticles and a small temperature gradient across the layer. The temperature gradient must be small anyway not to kill microorganisms, and the requirement of a dilute suspension ensures that the theory developed for oxytactic microorganisms in [10] and [11] holds. (A reasonable estimate would be that the temperature difference between the plates should not exceed 1 K.) As a result of this, Eq. (2) is recast as follows:

$$\rho_{f0}\left(\frac{\partial \mathbf{U}^*}{\partial t^*} + \mathbf{U}^*\cdot\nabla\mathbf{U}^*\right) = -\nabla^* p^* + \mu\nabla^{*2}\mathbf{U}^* + \left[\phi_0^*\rho_p + \left(1-\phi_0^*\right)\rho_{f0} - \rho_{f0}\beta\left(T^* - T_c^*\right) + \left(\rho_p - \rho_{f0}\right)\left(\phi^* - \phi_0^*\right) + n^*\theta\Delta\rho\right]\mathbf{g} \tag{3}$$

where ϕ^* is the nanoparticle volume fraction, and ϕ_0^* is the value of ϕ^* at the lower wall.

In a double-diffusive system, the thermal energy and solute conservation equations would normally include the Dufour-type and Soret-type diffusivities, respectively. However, in the particular water–oxygen system, these effects are negligible (these effects were neglected in [10,11] and [12]). The thermal energy equation for the nanofluid is

$$(\rho c)_f\left[\frac{\partial T^*}{\partial t^*} + \mathbf{U}^*\cdot\nabla^* T^*\right] = \nabla^*\cdot(k\nabla T^*) + (\rho c)_p\left[D_B\nabla^*\phi^*\cdot\nabla^* T^* + \frac{D_T}{T^*}\nabla^* T^*\cdot\nabla^* T^*\right] \tag{4}$$

where D_B and D_T are the Brownian and thermophoretic diffusion coefficients, respectively; and $(\rho c)_f$ and $(\rho c)_p$ are the volumetric heat capacities for the nanofluid and nanoparticles, respectively. It should be noted that nanofluids are characterized by enhanced heat and mass transfer [29]. However, based on the assumption that nanoparticle concentration is small, Eq. (4) is further simplified by neglecting the spatial variation of the nanofluid thermal conductivity k. Also, it is assumed that the temperature variation in the fluid is small compared with T_c^* and D_T/T^* is replaced by D_T/T_c^*.

The equation describing the conservation of the nanoparticles in the absence of chemical reactions is [25,26]:

$$\frac{\partial\phi^*}{\partial t^*} + \mathbf{U}^*\cdot\nabla\phi^* = \nabla^*\cdot\left[D_B\nabla\phi^* + \frac{D_T}{T^*}\nabla^* T^*\right] \tag{5}$$

The right-hand side of this equation includes the sum of two diffusion terms, which represent Brownian diffusion and thermophoresis. Equation (5) is further simplified by replacing D_T/T^* in the last term of this equation by D_T/T_c^*, similar to Eq. (4).

The conservation of microorganisms equation is based on the model of bioconvection in a suspension of oxytactic microorganisms developed in [10,11]:

$$\frac{\partial n^*}{\partial t^*} = -\nabla^*\cdot\mathbf{j}^* \tag{6}$$

In Eq. (6)

$$\mathbf{j}^* = n^*\mathbf{U}^* + n^*\mathbf{V}^* - D_{\mathrm{mo}}\nabla^* n^* \tag{7}$$

is the flux of microorganisms. The right-hand side of Eq. (7) represents the flux of microorganisms due to the macroscopic motion of the fluid, the directional swimming of microorganisms up the oxygen gradients, and a diffusive process that models all random motions of microorganisms. In Eq. (7), D_{mo} is the diffusivity of microorganisms.

Following [11], the average directional swimming velocity of a microorganism is approximated as

$$\mathbf{V}^* = bW_{\mathrm{mo}}\hat{H}(C)\nabla^* C \tag{8}$$

where b is the chemotaxis constant [m], and W_{mo} is the maximum cell swimming speed [m/s] (the product bW_{mo} is assumed to be constant). The dimensionless oxygen concentration, C, in Eq. (8) is defined as follows:

$$C = \frac{C^* - C^*_{\min}}{C^*_0 - C^*_{\min}} \tag{9}$$

where C^* is the dimensional oxygen concentration, C^*_0 is the upper-surface oxygen concentration (the upper surface is assumed to be open to atmosphere), and $C^*_{\min}$ is the minimum oxygen concentration that microorganisms need in order to be active. Since for the shallow layer $C > 0$ throughout the layer thickness, the Heaviside step function, $\hat{H}\,(C)$, in Eq. (8) is equal to unity.

The oxygen conservation equation is

$$\frac{\partial C}{\partial t^*} + \mathbf{U}^* \cdot \nabla^* C = D_S \nabla^{*2} C - \frac{\gamma n^*}{\Delta C} \tag{10}$$

where D_S is the diffusivity of oxygen, $-\gamma n^*/\Delta C$ describes the consumption of oxygen by the microorganisms in the fluid, and ΔC equals $C^*_0 - C^*_{\min}$. It has been assumed that the nanoparticles do not affect the transport of oxygen.

The temperature and the volumetric fraction of the nanoparticles are assumed to be constant on the boundaries. At the bottom of the layer, the boundary conditions are

$$w^* = 0, \quad \frac{\partial w^*}{\partial z^*} = 0, \quad T^* = T^*_h, \quad \phi^* = \phi^*_0, \quad \mathbf{j} \cdot \hat{\mathbf{k}} = 0, \quad \frac{\partial C^*}{\partial z^*} = 0 \quad \text{at} \quad z^* = H, \tag{11}$$

where T^*_h is the temperature at the lower wall, and $\hat{\mathbf{k}}$ is the vertically downward unit vector.

Two types of boundary conditions can be physically imposed at the upper surface; this boundary can be assumed either rigid or stress free (Fig. 1). If the upper surface is rigid, the boundary conditions imposed there are

$$w^* = 0, \quad \frac{\partial w^*}{\partial z^*} = 0, \quad T^* = T^*_c, \quad \phi^* = \phi^*_1, \quad \mathbf{j} \cdot \hat{\mathbf{k}} = 0, \quad C^* = C^*_0 \quad \text{at} \quad z^* = 0 \tag{12}$$

where ϕ^*_1 is the nanoparticle concentration at the upper wall.

If the upper surface is stress free, the second equation in (12) is replaced with the following equation:

$$\frac{\partial^2 w^*}{\partial z^{*2}} = 0 \tag{13}$$

In the dimensionless form, the governing equations are

$$\nabla \cdot \mathbf{U} = 0 \tag{14}$$

$$\frac{1}{\mathrm{Pr}}\left(\frac{\partial \mathbf{U}}{\partial t} + \mathbf{U} \cdot \nabla \mathbf{U}\right) = -\nabla p + \nabla^2 \mathbf{U} + \mathrm{Rm}\,\hat{\mathbf{k}} - \mathrm{Ra}T\hat{\mathbf{k}} + \mathrm{Rn}\phi\hat{\mathbf{k}} + \frac{\mathrm{Rb}}{\mathrm{Lb}} n\hat{\mathbf{k}} \tag{15}$$

$$\frac{\partial T}{\partial t} + \mathbf{U} \cdot \nabla T = \nabla^2 T + \frac{N_B}{\mathrm{Ln}} \nabla\phi \cdot \nabla T + \frac{N_A N_B}{\mathrm{Ln}} \nabla T \cdot \nabla T \tag{16}$$

$$\frac{\partial \phi}{\partial t} + \mathbf{U} \cdot \nabla \phi = \frac{1}{\mathrm{Ln}} \nabla^2 \phi + \frac{N_A}{\mathrm{Ln}} \nabla^2 T \tag{17}$$

$$\frac{\partial n}{\partial t} = -\nabla \cdot \left(n\mathbf{U} + n\mathbf{V} - \frac{1}{\mathrm{Lb}} \nabla n\right) \tag{18}$$

where $\mathbf{U} = (u, v, w)$ is the dimensionless nanofluid velocity, defined as $\mathbf{U}^* H/\alpha_f$ (α_f is the thermal diffusivity of a nanofluid, $k/(\rho c)_f$), and $\mathbf{V}$ is the dimensionless swimming velocity of a microorganism, $\mathbf{V}^* H/\alpha_f$, which is calculated as:

$$\mathbf{V} = \frac{\mathrm{Pe}}{\mathrm{Lb}} \hat{H}\,(C)\,\nabla C \tag{19a}$$

In Eq. (19a), Pe is the bioconvection Péclet number, which is defined as the ratio of a characteristic velocity due to oxytactic swimming to a characteristic velocity due to random, diffusive swimming:

$$\mathrm{Pe} = \frac{bW_{\mathrm{mo}}}{D_{\mathrm{mo}}} \tag{19b}$$

Finally, the dimensionless form of the oxygen conservation is

$$\frac{\partial C}{\partial t} + \mathbf{U}\cdot\nabla C = \frac{1}{\mathrm{Le}}\nabla^2 C - \hat{\beta} n \tag{20}$$

where

$$\hat{\beta} = \frac{\gamma H^2 n_0^*}{\Delta C \alpha_f} \tag{21}$$

In Eq. (21), n_0^* is the average number density of microorganisms (number density of microorganisms in a well-stirred suspension).

According to [11], the layer can be treated as shallow as long as the following condition is satisfied:

$$\hat{\beta} \le \frac{2\left(\exp\left(\mathrm{Pe}\right)-1\right)^{1/2}}{\mathrm{PeLe}} \tan^{-1}\left[\left(\exp\left(\mathrm{Pe}\right)-1\right)^{1/2}\right] \tag{22}$$

Since $\hat{\beta}$ is proportional to H^2, Eq. (22) gives the maximum layer depth for which the oxygen concentration at the bottom does not drop below C_{min}^*.

Dimensionless variables in Eqs. (14–20) are introduced as follows:

$$(x, y, z) = (x^*, y^*, z^*)/H, \quad t = t^*\alpha_f/H^2, \quad (u, v, w) = (u^*, v^*, w^*)H/\alpha_f \tag{23}$$

$$p = p^* H^2/\mu\alpha_f, \quad \phi = \frac{\phi^* - \phi_0^*}{\phi_1^* - \phi_0^*}, \quad T = \frac{T^* - T_c^*}{T_h^* - T_c^*}, \quad n = n^*/n_0^* \tag{24}$$

The dimensionless parameters in Eqs. (14–20) are

$$\mathrm{Pr} = \frac{\mu}{\rho_{f0}\alpha_f}, \quad \mathrm{Le} = \frac{\alpha_f}{D_S}, \quad \mathrm{Lb} = \frac{\alpha_f}{D_{\mathrm{mo}}}, \quad \mathrm{Ln} = \frac{\alpha_f}{D_B} \tag{25}$$

$$\mathrm{Ra} = \frac{\rho_{f0} g\beta H^3 (T_h^* - T_c^*)}{\mu\alpha_f}, \quad \mathrm{Rm} = \frac{\left[\rho_p\phi_0^* + \rho_{f0}(1-\phi_0^*)\right] g H^3}{\mu\alpha_f} \tag{26}$$

$$\mathrm{Rn} = \frac{(\rho_p - \rho_{f0})(\phi_1^* - \phi_0^*) g H^3}{\mu\alpha_f}, \quad \mathrm{Rb} = \frac{\Delta\rho g\theta n_0^* H^3}{\mu D_{\mathrm{mo}}} \tag{27}$$

$$N_A = \frac{D_T(T_h^* - T_c^*)}{D_B T_c^*(\phi_1^* - \phi_0^*)} \quad N_B = \frac{(\rho c)_p}{(\rho c)_f}\left(\phi_1^* - \phi_0^*\right) \tag{28}$$

In Eqs. (25–28), the parameter Le is the traditional Lewis number (the ratio of the Schmidt number to the Prandtl number Pr), Ln is the nanoparticle Lewis number, Lb is the bioconvection Lewis number, Ra is the thermal Rayleigh number, Rm is the basic-density Rayleigh number, Rn is the nanoparticle concentration Rayleigh number, and Rb is the bioconvection Rayleigh number. The parameter N_A is a modified diffusivity ratio (somewhat similar to the Soret parameter that arises in cross-diffusion phenomena in solutions), and N_B is a modified particle-density increment; g is gravity.

The boundary conditions for Eqs. (14–18) and (20) are imposed as follows. It is assumed that the temperature and the volumetric fraction of the nanoparticles are constant on the boundaries. The dimensionless form of boundary conditions (11, 12) for the rigid upper wall is

$$w = 0, \quad \frac{\partial w}{\partial z} = 0, \quad T = 1, \quad \phi = 0, \quad \frac{\mathrm{d}n}{\mathrm{d}z} = 0, \quad \frac{\partial C}{\partial z} = 0 \quad \text{at} \quad z = 1, \tag{29}$$

$$w = 0, \quad \frac{\partial w}{\partial z} = 0, \quad T = 0, \quad \phi = 1, \quad \mathrm{Pe}\, n\frac{\mathrm{d}C}{\mathrm{d}z} - \frac{\mathrm{d}n}{\mathrm{d}z} = 0, \quad C = 1 \quad \text{at} \quad z = 0. \tag{30}$$

If the upper surface is stress free, the second equation in (30) is replaced with the following equation:

$$\frac{\partial^2 w}{\partial z^2} = 0 \tag{31}$$

3 Basic state

In the basic state, the solution is of the form

$$\mathbf{U} = 0, \quad p = p_b(z), \quad T = T_b(z), \quad \phi = \phi_b(z), \quad n = n_b(z), \quad C = C_b(z) \tag{32}$$

Utilizing Eq. (32), Eqs. (15–18) and (20) are simplified as

$$-\frac{\mathrm{d}p_b}{\mathrm{d}z} + \mathrm{Rm} - \mathrm{Ra}T_b + \mathrm{Rn}\phi_b + \frac{\mathrm{Rb}}{\mathrm{Lb}} n_b = 0 \tag{33}$$

$$\frac{\mathrm{d}^2 T_b}{\mathrm{d}z^2} + \frac{N_B}{\mathrm{Ln}} \frac{\mathrm{d}\phi_b}{\mathrm{d}z} \frac{\mathrm{d}T_b}{\mathrm{d}z} + \frac{N_A N_B}{\mathrm{Ln}} \left(\frac{\mathrm{d}T_b}{\mathrm{d}z} \right)^2 = 0 \tag{34}$$

$$\frac{\mathrm{d}^2 \phi_b}{\mathrm{d}z^2} + N_A \frac{\mathrm{d}^2 T_b}{\mathrm{d}z^2} = 0 \tag{35}$$

$$\mathrm{Pe} \frac{\mathrm{d}C}{\mathrm{d}z} \frac{\mathrm{d}n}{\mathrm{d}z} + \mathrm{Pe}\, n \frac{\mathrm{d}^2 C}{\mathrm{d}z^2} - \frac{\mathrm{d}^2 n}{\mathrm{d}z^2} = 0 \tag{36}$$

$$\frac{\mathrm{d}^2 C}{\mathrm{d}z^2} - \hat{\beta} \mathrm{Le}\, n = 0 \tag{37}$$

Using boundary conditions (29) and (30), Eq. (35) is integrated twice to give

$$\phi_b = -N_A T_b - (1 - N_A) z + 1 \tag{38}$$

The substitution of Eq. (38) into Eq. (34) gives

$$\frac{\mathrm{d}^2 T_b}{\mathrm{d}z^2} - \frac{(1 - N_A)\, N_B}{\mathrm{Ln}} \frac{\mathrm{d}T_b}{\mathrm{d}z} = 0 \tag{39}$$

The solution of Eq. (39) satisfying Eqs. (29) and (30) is

$$T_b\,(z) = \frac{\exp\left[\frac{(1-N_A)N_B}{\mathrm{Ln}} z\right] - 1}{\exp\left[\frac{(1-N_A)N_B}{\mathrm{Ln}}\right] - 1} \tag{40}$$

Eq. (38) then gives

$$\phi_b\,(z) = -N_A \frac{\exp\left[\frac{(1-N_A)N_B}{\mathrm{Ln}} z\right] - 1}{\exp\left[\frac{(1-N_A)N_B}{\mathrm{Ln}}\right] - 1} - (1 - N_A) z + 1 \tag{41}$$

For a typical alumina/water nanofluid, based on the data published in Buongiorno [25], the following dimensional parameter values are utilized: $\phi_0^* = 0.01$, $\alpha_f = 2 \times 10^{-7}\,\mathrm{m^2/s}$, $D_B = 4 \times 10^{-11}\,\mathrm{m^2/s}$, $\mu = 10^{-3}\mathrm{Pa\,s}$, and $\rho_{f0} = 10^3\,\mathrm{kg/m^3}$. The thermophoretic diffusion coefficient, D_T, is estimated as $\tau \frac{\mu}{\rho} \phi_0^*$, where, according to [25], τ is estimated as 0.006. This results in $D_T = 6 \times 10^{-11}\,\mathrm{m^2/s}$. The nanoparticle Lewis number is then estimated as $\mathrm{Ln} = 5.0 \times 10^3$. The modified diffusivity ratio, N_A, and the modified particle-density increment, N_B, depend on the temperature difference between the lower and the upper plates and on the nanoparticle fraction decrement. Assuming that $T_h^* - T_c^* = 1\,\mathrm{K}$, $\phi_1^* - \phi_0^* = 0.001$, and $T_c^* = 300\,\mathrm{K}$, gives the following estimates: $N_A = 5$ and $N_B = 7.5 \times 10^{-4}$.

Figure 2a displays $\phi_b(z)$ and $T_b\,(z)$ computed for these parameter values. Figure 2a suggests that in the limit as Ln becomes large, Eqs. (40) and (41) can be simplified as:

$$T_b = 1 - z, \tag{42}$$

$$\phi_b = z \tag{43}$$

The solutions for $C_b(z)$ and $n_b(z)$ are found in [10] and [11] as

$$C_b(z) = 1 - \frac{2}{\mathrm{Pe}} \ln\left(\frac{\cos\{A_1(1-z)/2\}}{\cos\{A_1/2\}}\right) \tag{44}$$

$$n_b(z) = \frac{A_1^2}{2\mathrm{Pe}\hat{\beta}\mathrm{Le}} \sec^2\left(\frac{A_1(1-z)}{2}\right) \tag{45}$$

where A_1 is the smallest positive root of the transcendental equation

$$\tan\left(\frac{A_1}{2}\right) = \mathrm{Pe}\frac{\hat{\beta}\mathrm{Le}}{A_1} \tag{46}$$

Figure 2b shows plots of $n_b(z)$ and $C_b(z)$; these plots are computed for Le = 94, Pe = 37, and $\hat{\beta} = 0.46$ (these parameter values are justified in Sect. 5.1.2 below). $C_b(z)$ grows monotonically when z is increasing and reaches the value of one at the upper boundary, in accordance with Eq. (30). $n_b(z)$ also monotonically increases (due to microorganisms upswimming); diffusion is the only mechanism that prevents all microorganisms from accumulating at the top of the layer (diffusion models stochastic motions of microorganisms; due to these motions, the diffusivity of microorganisms D_{mo} is much larger than it would be if microorganisms were just solid particles with the same diameter).

The remainder of the basic solution is obtained by integrating Eq. (33) to obtain p_b.

4 Linear instability analysis

For the linear instability analysis, perturbations are superimposed on the basic solution, according to the following equation:

$$\begin{aligned}[\mathbf{U}, T, \phi, n, C, p] &= [0, T_b(z), \phi_b(z), n_b(z), C_b(z), p_b(z)] \\ &+ \varepsilon\left[\mathbf{U}'(t,x,y,z), T'(t,x,y,z), \phi'(t,x,y,z), n'(t,x,y,z), C'(t,x,y,z), p'(t,x,y,z)\right]\end{aligned} \tag{47}$$

Upon the substitution of Eq. (47) into Eqs. (14)–(18) and (20), the linearization of the results, and the utilization of Eqs. (42) and (43), the following equations for the perturbation quantities are obtained:

$$\nabla \cdot \mathbf{U}' = 0 \tag{48}$$

$$\frac{1}{\mathrm{Pr}}\frac{\partial \mathbf{U}'}{\partial t} = -\nabla p' + \nabla^2 \mathbf{U}' - \mathrm{Ra}T'\hat{\mathbf{k}} + \mathrm{Rn}\phi'\hat{\mathbf{k}} + \frac{\mathrm{Rb}}{\mathrm{Lb}}n'\hat{\mathbf{k}} \tag{49}$$

$$\frac{\partial T'}{\partial t} + w' = \nabla^2 T' + \frac{N_B}{\mathrm{Ln}}\left(\frac{\partial \phi'}{\partial z} - \frac{\partial T'}{\partial z}\right) + \frac{2N_A N_B}{\mathrm{Ln}}\frac{\partial T'}{\partial z} \tag{50}$$

$$\frac{\partial \phi'}{\partial t} - w' = \frac{1}{\mathrm{Ln}}\nabla^2\phi' + \frac{N_A}{\mathrm{Ln}}\nabla^2 T' \tag{51}$$

$$\frac{\partial n'}{\partial t} + w'\frac{\mathrm{d}n_b}{\mathrm{d}z} + \frac{\mathrm{Pe}}{\mathrm{Lb}}\left(\frac{\partial C'}{\partial z}\frac{\mathrm{d}n_b}{\mathrm{d}z} + \frac{\mathrm{d}C_b}{\mathrm{d}z}\frac{\partial n'}{\partial z} + n'\frac{\mathrm{d}^2 C_b}{\mathrm{d}z^2} + n_b\nabla^2 C'\right) = \frac{1}{\mathrm{Lb}}\nabla^2 n' \tag{52}$$

$$\frac{\partial C'}{\partial t} + w'\frac{\mathrm{d}C_b}{\mathrm{d}z} = \frac{1}{\mathrm{Le}}\nabla^2 C' - \hat{\beta}n' \tag{53}$$

Following [26], Eq. (49) is then operated with $\hat{\mathbf{k}} \cdot$ curl curl [where curl curl $\mathbf{A} = \nabla \times (\nabla \times \mathbf{A})$], and the use is made of the identity $\nabla \times (\nabla \times \mathbf{A}) = \nabla(\nabla \cdot \mathbf{A}) - \nabla^2\mathbf{A}$ (which is valid for any arbitrary vector field $\mathbf{A}$) together with Eq. (48). This results in the elimination of the pressure and horizontal components of velocity, and Eqs. (48) and (49) reduce to the following single scalar equation:

$$\frac{1}{\mathrm{Pr}}\frac{\partial}{\partial t}\nabla^2 w' - \nabla^4 w' = -\mathrm{Ra}\nabla_H^2 T' + \mathrm{Rn}\nabla_H^2\phi' + \frac{\mathrm{Rb}}{\mathrm{Lb}}\nabla_H^2 n' \tag{54}$$

where ∇_H^2 is the two-dimensional Laplacian operator in the horizontal plane, and $\nabla^4 w'$ is the Laplacian of the Laplacian of w'.

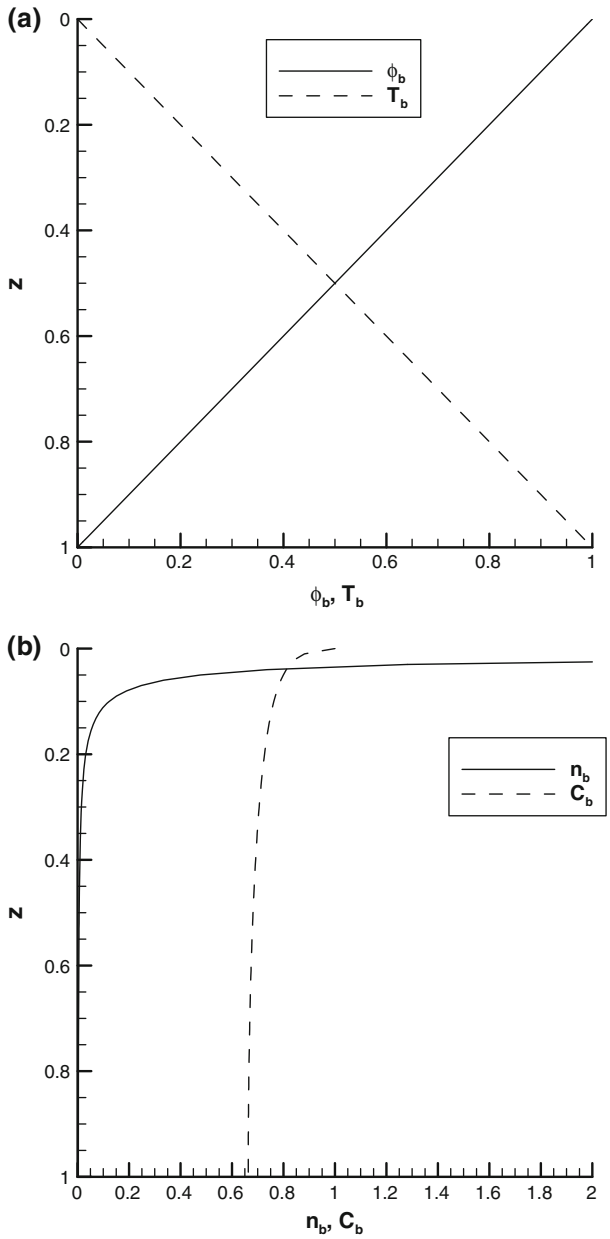

Fig. 2 Solution in the basic state: **a** $\phi_b\,(z)$, $T_b\,(z)$; **b** $n_b\,(z)$, $C_b\,(z)$

At the bottom wall, the boundary conditions for disturbances are:

$$w' = 0, \quad \frac{\partial w'}{\partial z} = 0, \quad T' = 0, \quad \phi' = 0, \quad \frac{\mathrm{d}n'}{\mathrm{d}z} = 0, \quad \frac{\mathrm{d}C'}{\mathrm{d}z} = 0 \quad \text{at} \quad z = 1 \tag{55}$$

If the upper wall is rigid, the boundary conditions for disturbances at the upper wall are

$$w' = 0, \quad \frac{\partial w'}{\partial z} = 0, \quad T' = 0, \quad \phi' = 0, \quad \mathrm{Pe}\left[n_b \frac{\mathrm{d}C'}{\mathrm{d}z} + \frac{\mathrm{d}C_b}{\mathrm{d}z} n'\right] - \frac{\mathrm{d}n'}{\mathrm{d}z} = 0, \quad C' = 0 \quad \text{at} \quad z = 0 \tag{56}$$

If the upper boundary is stress free, the second equation in Eq. (56) is replaced by

$$\frac{\partial^2 w'}{\partial z^2} = 0 \quad \text{at } z = 0 \tag{57}$$

A linear boundary-value problem composed of differential Eqs. (50–54) and boundary conditions (55, 56), or (57) is solved by the method of normal modes. A normal mode expansion is introduced as follows:

$$\left[w', T', \phi', n', C'\right] = [W(z), \Theta(z), \Phi(z), N(z), \Xi(z)] f(x, y) \exp(st), \tag{58}$$

The function $f(x, y)$ satisfies the following equation:

$$\frac{\partial^2 f}{\partial x^2} + \frac{\partial^2 f}{\partial y^2} = -m^2 f \tag{59}$$

where m is the dimensionless horizontal wave number.

In Eq. (58), s is a dimensionless growth factor; for neutral stability, the real part of s is zero, so it is written $s = i\omega$, where ω is a dimensionless frequency (it is a real number).

Equation (58) is then substituted into Eqs. (54) and (50–53) (in that order), and the use is made of Eq. (59). This procedure leads to the following equations for the amplitudes, W, Θ, Φ, N, and Ξ:

$$\frac{\mathrm{d}^4 W}{\mathrm{d}z^4} - 2m^2 \frac{\mathrm{d}^2 W}{\mathrm{d}z^2} + m^4 W - \frac{s}{\mathrm{Pr}} \frac{\mathrm{d}^2 W}{\mathrm{d}z^2} + m^2 \frac{s}{\mathrm{Pr}} W + \mathrm{Ra} m^2 \Theta - \mathrm{Rn} m^2 \Phi - \frac{\mathrm{Rb}}{\mathrm{Lb}} m^2 N = 0 \tag{60}$$

$$-W + \frac{\mathrm{d}^2 \Theta}{\mathrm{d}z^2} - \frac{N_B}{\mathrm{Ln}} \frac{\mathrm{d}\Theta}{\mathrm{d}z} + \frac{2 N_A N_B}{\mathrm{Ln}} \frac{\mathrm{d}\Theta}{\mathrm{d}z} - \left(m^2 + s\right) \Theta + \frac{N_B}{\mathrm{Ln}} \frac{\mathrm{d}\Phi}{\mathrm{d}z} = 0 \tag{61}$$

$$-W + \frac{N_A}{\mathrm{Ln}} m^2 \Theta + \frac{1}{\mathrm{Ln}} m^2 \Phi + s\Phi - \frac{N_A}{\mathrm{Ln}} \frac{\mathrm{d}^2 \Theta}{\mathrm{d}z^2} - \frac{1}{\mathrm{Ln}} \frac{\mathrm{d}^2 \Phi}{\mathrm{d}z^2} = 0 \tag{62}$$

$$\begin{aligned} &-2A_1 \mathrm{LePe}\hat{\beta} \tan\left[\frac{1}{2} A_1 (1 - z)\right] \frac{\mathrm{d}N}{\mathrm{d}z} - A_1^3 \sec^2\left[\frac{1}{2} A_1 (1 - z)\right] \tan\left[\frac{1}{2} A_1 (1 - z)\right] \left(\mathrm{Lb} W + \mathrm{Pe} \frac{\mathrm{d}\Xi}{\mathrm{d}z}\right) \\ &+ 2\mathrm{LePe}\hat{\beta} \left(m^2 N - \frac{\mathrm{d}^2 N}{\mathrm{d}z^2}\right) + A_1^2 \mathrm{Pe} \sec^2\left[\frac{1}{2} A_1 (1 - z)\right] \left(\hat{\beta} \mathrm{Le} N - m^2 \Xi + \frac{\mathrm{d}^2 \Xi}{\mathrm{d}z^2}\right) \\ &+ 2\mathrm{LbLePe} s \hat{\beta} N = 0 \end{aligned} \tag{63}$$

$$\hat{\beta} N - \frac{A_1 \tan\left(\frac{1}{2} A_1 (1 - z)\right) W}{\mathrm{Pe}} + \frac{m^2 \Xi}{\mathrm{Le}} + s\Xi - \frac{1}{\mathrm{Le}} \frac{\mathrm{d}^2 \Xi}{\mathrm{d}z^2} = 0 \tag{64}$$

At the bottom wall the boundary conditions for the amplitudes are

$$W = 0, \quad \frac{\mathrm{d}W}{\mathrm{d}z} = 0, \quad \Theta = 0, \quad \Phi = 0, \quad \frac{\mathrm{d}N}{\mathrm{d}z} = 0, \quad \frac{\mathrm{d}\Xi}{\mathrm{d}z} = 0 \quad \text{at} \quad z = 1, \tag{65}$$

If the upper wall is rigid, the boundary conditions for the amplitudes at the upper wall are

$$W = 0, \quad \frac{\mathrm{d}W}{\mathrm{d}z} = 0, \quad \Theta = 0, \quad \Phi = 0, \quad \mathrm{Pe}\left[n_b|_{z=0} \frac{\mathrm{d}\Xi}{\mathrm{d}z} + \frac{\mathrm{d}C_b}{\mathrm{d}z}\bigg|_{z=0} N\right] - \frac{\mathrm{d}N}{\mathrm{d}z} = 0, \quad \Xi = 0 \quad \text{at} \quad z = 0, \tag{66}$$

For the stress-free upper surface, the second equation in (66) is replaced by

$$\frac{\mathrm{d}^2 W}{\mathrm{d}z^2} = 0 \quad \text{at} \quad z = 0 \tag{67}$$

By letting $\Xi \to \hat{\beta}\bar{\Xi}$, the system (60–64) depends on the product $\varpi = \mathrm{Pe}\hat{\beta}$ rather than on Pe and $\hat{\beta}$ individually:

$$\frac{\mathrm{d}^4 W}{\mathrm{d}z^4} - 2m^2 \frac{\mathrm{d}^2 W}{\mathrm{d}z^2} + m^4 W - \frac{s}{\mathrm{Pr}} \frac{\mathrm{d}^2 W}{\mathrm{d}z^2} + m^2 \frac{s}{\mathrm{Pr}} W + \mathrm{Ra} m^2 \Theta - \mathrm{Rn} m^2 \Phi - \frac{\mathrm{Rb}}{\mathrm{Lb}} m^2 N = 0 \tag{68}$$

$$-W + \frac{\mathrm{d}^2 \Theta}{\mathrm{d}z^2} - \frac{N_B}{\mathrm{Ln}} \frac{\mathrm{d}\Theta}{\mathrm{d}z} + \frac{2 N_A N_B}{\mathrm{Ln}} \frac{\mathrm{d}\Theta}{\mathrm{d}z} - \left(m^2 + s\right) \Theta + \frac{N_B}{\mathrm{Ln}} \frac{\mathrm{d}\Phi}{\mathrm{d}z} = 0 \tag{69}$$

$$-W + \frac{N_A}{\mathrm{Ln}} m^2 \Theta + \frac{1}{\mathrm{Ln}} m^2 \Phi + s\Phi - \frac{N_A}{\mathrm{Ln}} \frac{\mathrm{d}^2 \Theta}{\mathrm{d}z^2} - \frac{1}{\mathrm{Ln}} \frac{\mathrm{d}^2 \Phi}{\mathrm{d}z^2} = 0 \tag{70}$$

$$-2A_1\mathrm{Le}\varpi\tan\left[\frac{1}{2}A_1(1-z)\right]\frac{\mathrm{d}N}{\mathrm{d}z}-A_1^3\sec^2\left[\frac{1}{2}A_1(1-z)\right]\tan\left[\frac{1}{2}A_1(1-z)\right]\left(\mathrm{Lb}W+\varpi\frac{\mathrm{d}\bar{\Xi}}{\mathrm{d}z}\right)$$
$$+2\mathrm{Le}\varpi\left(m^2N-\frac{\mathrm{d}^2N}{\mathrm{d}z^2}\right)+A_1^2\varpi\sec^2\left[\frac{1}{2}A_1(1-z)\right]\left(\mathrm{Le}N-m^2\bar{\Xi}+\frac{\mathrm{d}^2\bar{\Xi}}{\mathrm{d}z^2}\right)+2\mathrm{LbLe}\varpi sN=0 \tag{71}$$

$$\varpi N-A_1\tan\left(\frac{1}{2}A_1(1-z)\right)W+\frac{\varpi m^2\bar{\Xi}}{\mathrm{Le}}+\varpi s\bar{\Xi}-\frac{\varpi}{\mathrm{Le}}\frac{\mathrm{d}^2\bar{\Xi}}{\mathrm{d}z^2}=0 \tag{72}$$

where Eq. (46) for A_1 now becomes

$$\tan\left(\frac{A_1}{2}\right)=\frac{\varpi\mathrm{Le}}{A_1} \tag{73}$$

Equations (68)–(72) with boundary conditions given by Eqs. (65), (66), or (67) are solved by using a Galerkin-type weighted residuals method. First, the trial functions, $W_p, \Theta_p, \Phi_p, N_p, \bar{\Xi}_p (p = 1, 2, \ldots, N)$, which must satisfy boundary conditions, are chosen. Then, the following expressions are formed:

$$W=\sum_{p=1}^{N}\hat{A}_pW_p,\quad \Theta=\sum_{p=1}^{N}\hat{B}_p\Theta_p,\quad \Phi=\sum_{p=1}^{N}\hat{C}_p\Phi_p,\quad N=\sum_{p=1}^{N}\hat{D}_pN_p,\quad \bar{\Xi}=\sum_{p=1}^{N}\hat{E}_p\bar{\Xi}_p \tag{74}$$

These expressions are substituted into Eqs. (68)–(72), and the residuals are made orthogonal to the trial functions. This gives a system of $5N$ linear equations in $5N$ unknowns $\hat{A}_p, \hat{B}_p, \hat{C}_p, \hat{D}_p, \hat{E}_p (p = 1, 2, \ldots, N)$. The vanishing of the determinant of coefficients produces an eigenvalue equation for this linear system of equations, and Ra can be regarded as an eigenvalue.

5 Results and Discussion

5.1 Rigid–rigid boundaries

5.1.1 Trial functions

First, the case where both the lower and upper boundaries are rigid is investigated. The physical justification for the imposition of a rigid-wall condition at the upper boundary is modeling the situation when the upswimming microorganisms form a packed layer at the upper surface. A one-term Galerkin method is utilized. Following a standard Galerkin procedure [30], the trial functions that satisfy the boundary conditions (65) and (66) are chosen as

$$W_1=z^2(1-z)^2,\quad \Theta_1=z(1-z),\quad \Phi_1=z(1-z),\quad N_1=1+\alpha\left(z-\frac{1}{2}z^2\right),$$
$$\bar{\Xi}_1=z-\frac{1}{2}z^2 \tag{75}$$

where

$$\alpha=\frac{A_1(A_1-\mathrm{Le}\sin A_1)}{\mathrm{Le}(1+\cos A_1)} \tag{76}$$

and A_1 is given by Eq. (73).

5.1.2 Non-oscillatory instability

Due to complexity of the problem, the analysis is restricted to non-oscillatory instability. On physical grounds, the oscillatory instability is possible when Rn is negative (which corresponds to a bottom-heavy, stabilizing, nanoparticle distribution), and Ra is positive (which corresponds to heating from the bottom). In this case, the destabilizing effect of the temperature gradient and the destabilizing effect from upswimming of oxytactic microorganisms compete with the stabilizing effect of the nanoparticle distribution.

For the case of non-oscillatory instability, $\omega = 0$. The eigenvalue equation in this case is

$$\mathrm{Ra} + (N_A + \mathrm{Ln})\,\mathrm{Rn} + F_1 \mathrm{Rb} = F_2 \tag{77}$$

where F_1 is a function of Lb, Le, ϖ, and m, and F_2 is a function of m only. Functions F_1 and F_2 are given in the Appendix [see Eqs. (A1) and (A2)]. If Rb = 0, which physically corresponds to the situation when the suspension does not contain any microorganisms, only the base fluid and nanoparticles, the third term on the left-hand side of Eq. (77) vanishes and the right-hand side of Eq. (77) takes the minimum value of 1,750 at $m = 3.116$. Thus, in the case of Rb = 0 Eq. (77) collapses to the following equation reported in [26]:

$$\mathrm{Ra} + (N_A + \mathrm{Ln})\,\mathrm{Rn} = 1750 \tag{78}$$

For the case of a regular fluid (not a nanofluid) Rn = 0 and Eq. (78) gives $\mathrm{Ra_{cr}} = 1,750$. The obtained critical value of Ra is 2.5% greater than the exact value of 1,707.762 for the critical Rayleigh number for the classical Rayleigh–Bérnard problem [31]. The corresponding critical value of $m = 3.116$ is within 0.03% of the exact critical value of $m = 3.117$ [31]. This gives an estimate of the expected accuracy of the one-term Galerkin approximation.

Based on [25], the following parameter values for a typical alumina/water nanofluid are utilized: $\phi_0^* = 0.01$, $\rho_{f0} = 10^3\,\mathrm{kg/m^3}$, $\rho_p = 4\times10^3\,\mathrm{kg/m^3}$, $(\rho c)_p = 3.1\times10^6\,\mathrm{J/m^3}$, $\alpha_f = 2\times10^{-7}\,\mathrm{m^2/s}$, $D_B = 4\times10^{-11}\,\mathrm{m^2/s}$, $D_T = 6\times10^{-11}\,\mathrm{m^2/s}$, and $\mu = 10^{-3}\,\mathrm{Pa\,s}$. It is also assumed that $\phi_1^* - \phi_0^* = 0.001$, $\beta = 3.4\times10^{-3}\,1/\mathrm{K}$, $(\rho c)_f = 4\times10^6\,\mathrm{J/m^3}$, $T_h^* - T_c^* = 1\,\mathrm{K}$, and $T_c^* = 300\,\mathrm{K}$. Based on the data presented in [10] and [11] for soil bacterium *Bacillus subtilis*, the following data for these microorganisms are used: $D_{\mathrm{mo}} = 1.3\times10^{-10}\,\mathrm{m^2/s}$, $D_S = 2.12\times10^{-9}\,\mathrm{m^2/s}$, $\Delta\rho = 100\,\mathrm{kg/m^3}$, $n_0^* = 10^{15}\,\mathrm{cells/m^3}$, $\theta = 10^{-18}\,\mathrm{m^3}$, and $H = 2.5\times10^{-3}\,\mathrm{m}$ (or 2.5 mm, this is a typical depth of a shallow layer; this size is also typical for a microdevice). Also, according to [11], for *Bacillus subtilis* dimensionless parameters can be estimated as follows: $\mathrm{Pe} = 15H$, $\hat{\beta} = 7H^2/\mathrm{Le}$, where the layer depth, H, must be given in mm.

This results in the following values of dimensionless parameters: $\hat{\beta} = 0.46$, Pr = 5.0, Le = 94, $\mathrm{Ln} = 5.0\times10^3$, $\mathrm{Lb} = 1.5\times10^3$, Pe = 37, $\mathrm{Ra} = 2.7\times10^3$, $\mathrm{Rm} = 8.0\times10^5$, $\mathrm{Rn} = 2.3\times10^3$, $\mathrm{Rb} = 1.2\times10^5$, $N_A = 5$, $N_B = 7.5\times10^{-4}$, and $\varpi = 17$. The values of Ra and Rb can be controlled by changing the temperature difference between the plates and the cell concentration, respectively. For these numerical values, A_1 defined by Eq. (73) is close to π.

For Fig. 3, which displays the results for non-oscillatory convection for the rigid–rigid boundaries, the following values of dimensionless parameters are utilized: $\mathrm{Lb} = 1.5\times10^3$, Le = 94, $\mathrm{Ln} = 5.0\times10^3$, $\varpi = 17$, $N_A = 5$. This leads to $A_1 = 3.14$ and $\alpha = 1.20\times10^4$. Rb is assumed to take three values: 0, 1.2×10^5, and 2.4×10^5, and Rn is changing in the range between -1.2 and 1.2. Figure 3a shows that for any fixed value of Rb, the curve representing the instability boundary for non-oscillatory convection is a straight line in the ($\mathrm{Ra_{cr}}$, Rn) plane. The definition of Rn given by Eq. (27) is such that positive Rn corresponds to a top-heavy nanoparticle distribution and negative Rn corresponds to a bottom-heavy nanoparticle distribution. The effect of nanoparticles can therefore be either stabilizing or destabilizing, depending on whether the basic nanoparticle distribution is bottom-heavy or top-heavy. The increase in Rn produces the destabilizing effect and reduces the critical value of Ra. Oxytactic microorganisms are heavier than water, therefore Rb is always expected to be positive. Since the microorganisms swim on average in the upward direction, their presence produces a destabilizing effect and reduces the critical value of Ra. Rb can be increased, for example, by increasing the average concentration of microorganisms in the suspension. Figure 3b shows that the corresponding critical value of the wave number is independent of Rn but depends on Rb; it increases markedly when Rb is increased.

Figure 4 is computed for Le = 94, $\mathrm{Ln} = 5.0\times10^3$, $N_A = 5$, $\mathrm{Rb} = 1.2\times10^5$, and Rn = 1. Figure 4a shows $\mathrm{Ra_{cr}}$ versus ϖ for three values of Lb: 500, 1,500, and 4,500. There are clear minima on all three curves. It should be noted that dependences of Rayleigh numbers on ϖ in oxytactic bioconvection problems typically exhibit minima. For example, a minimum on a curve exhibiting a dependence of $\mathrm{Rb_{cr}}$ on ϖ was found in [11] for the case of pure bioconvection (see Fig. 6a in [11]) and in [16] for bio-thermal convection (see Figs. 3a

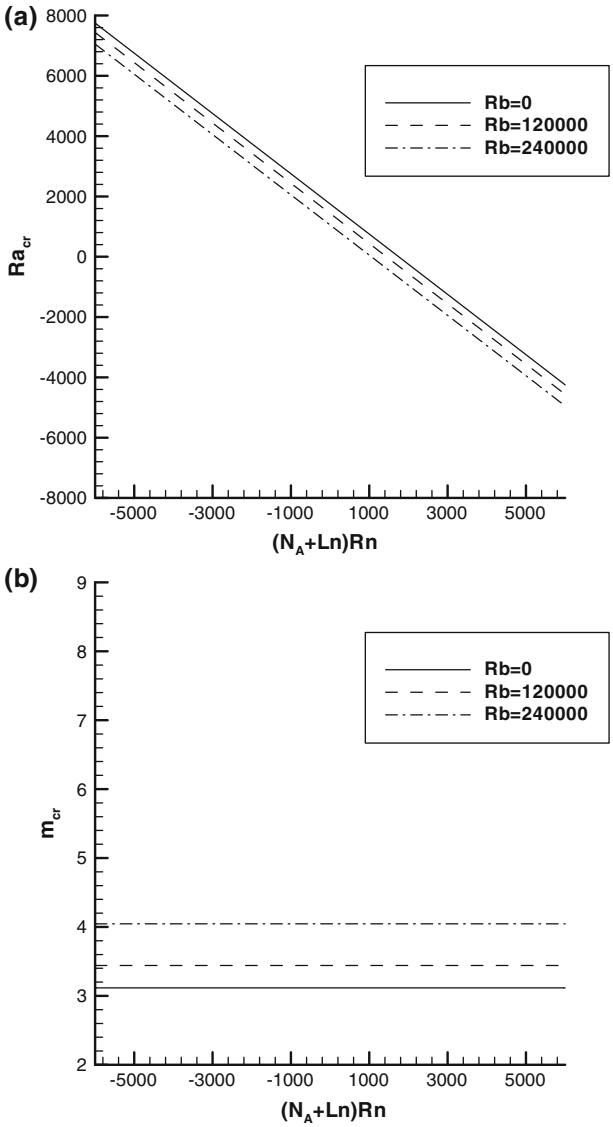

Fig. 3 The case of rigid upper and lower walls: **a** Non-oscillatory instability boundaries in the (Ra_{cr}, Rn) plane for various values of the bioconvection Rayleigh number, Rb. **b** Critical wavenumber in the (Ra_{cr}, Rn) plane for various values of Rb

and 4a in [16]). It is easy to explain the initial decrease in Ra_{cr} with ϖ; indeed, as shown in [11], ϖ can be interpreted as a depth parameter, and larger values of ϖ correspond to a steeper (and thus more unstable) free-surface density gradient in the basic state due to concentration of oxytactic microorganisms. However, a more elaborate physics must apparently be involved for explaining the increase in a critical Rayleigh number for large values of ϖ, see [11]. Figure 4a also shows that the effect of increasing the bioconvection Lewis number Lb is to increase Ra_{cr}. Figure 4b shows that the dependence of the corresponding critical wave number m_{cr} on ϖ exhibits a maximum, which is in agreement with the results displayed in Fig. 6b in [11].

Figure 5 is computed for $Lb = 1.5 \times 10^3$, $\varpi = 17$, $N_A = 5$, $Rb = 1.2 \times 10^5$, and Rn = 1. Figure 5a shows Ra_{cr} versus Ln for three values of Le: 50, 100, and 1,000. According to Eq. (77), the variation of Ra_{cr} with Ln is linear and depends on the sign of Rn. Since Fig. 5 is computed for a top-heavy, destabilizing distribution of nanoparticles ($Rn > 0$), the effect of increasing Ln in Fig. 5a is destabilizing. Physically, a large value of Ln corresponds to a small value of the Brownian diffusion coefficient of nanoparticles D_B. A smaller value of D_B corresponds to a more non-uniform, more top-heavy distribution of nanoparticles, which corresponds to a more unstable system. Figure 5a also shows that a decrease in Le produces a small destabilizing effect

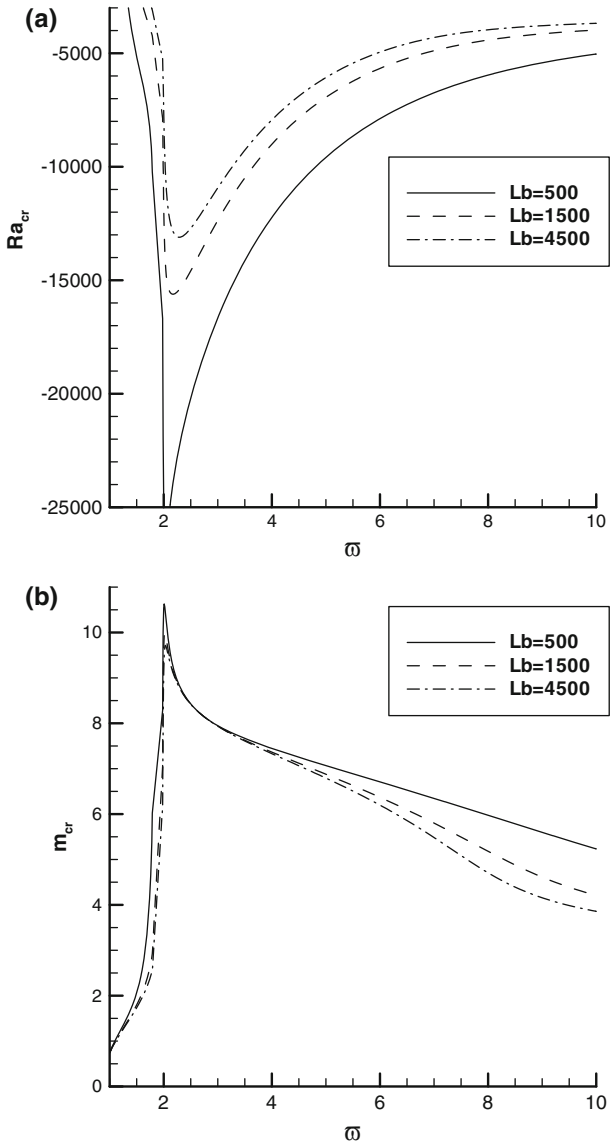

Fig. 4 The case of rigid upper and lower walls: **a** $\mathrm{Ra}_{\mathrm{cr}}$ versus the depth parameter ϖ for various values of the bioconvection Lewis number Lb. **b** m_{cr} versus ϖ for various values of Lb

on the system, more significant at smaller values of Le. According to Fig. 5b, the corresponding critical wave number is independent of Ln and increases slightly when Le is decreased.

5.2 Rigid-free boundaries

5.2.1 Trial functions

Next, the case when the lower boundary is rigid and the upper boundary is free is studied. For the case of a free top boundary, W_1 is replaced by

$$W_1 = z - 3z^3 + 2z^4 \tag{79}$$

and the rest of the trial functions is still given by Eq. (75).

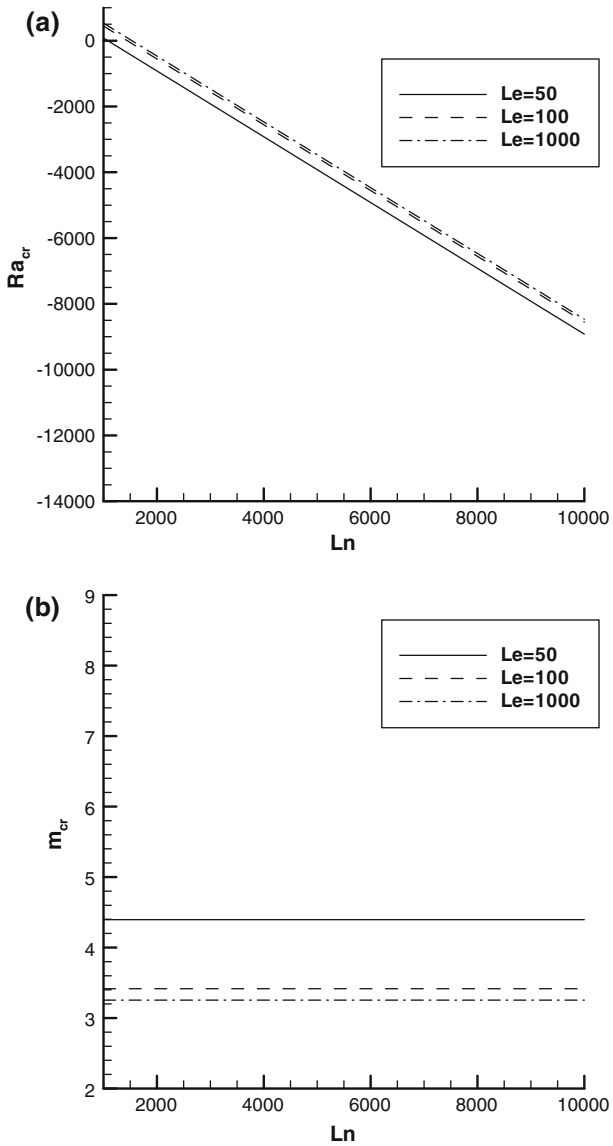

Fig. 5 The case of rigid upper and lower walls: **a** $\mathrm{Ra_{cr}}$ versus the nanoparticle Lewis number Ln for various values of the traditional Lewis number Le. **b** m_{cr} versus Ln for various values of Le

5.2.2 Non-oscillatory instability

Again, for the case of non-oscillatory instability, $\omega = 0$. The eigenvalue equation for this case is

$$\mathrm{Ra} + (N_A + \mathrm{Ln})\,\mathrm{Rn} + F_3\mathrm{Rb} = F_4 \tag{80}$$

where F_3 is a function of Lb, Le, ϖ, and m, and F_4 is a function of m only. Functions F_3 and F_4 are given in the Appendix [see Eqs. (A9) and (A10)].

If Rb = 0, which physically corresponds to the situation when the suspension does not contain any microorganisms, only the base fluid and nanoparticles, the third term on the left-hand side of Eq. (80) vanishes and the right-hand side of Eq. (80) takes the minimum value of 1,139 at $m = 2.670$. Thus, in the case of Rb = 0, Eq. (80) collapses to the following equation reported in [26]

$$\mathrm{Ra} + (N_A + \mathrm{Ln})\,\mathrm{Rn} = 1139 \tag{81}$$

For the case of a regular fluid (not a nanofluid), Rn = 0 and Eq. (81) gives $\mathrm{Ra_{cr}} = 1139$. The obtained critical value of Ra is 3.48% greater than the exact value of 1,100.65 for the critical Rayleigh number for the classical

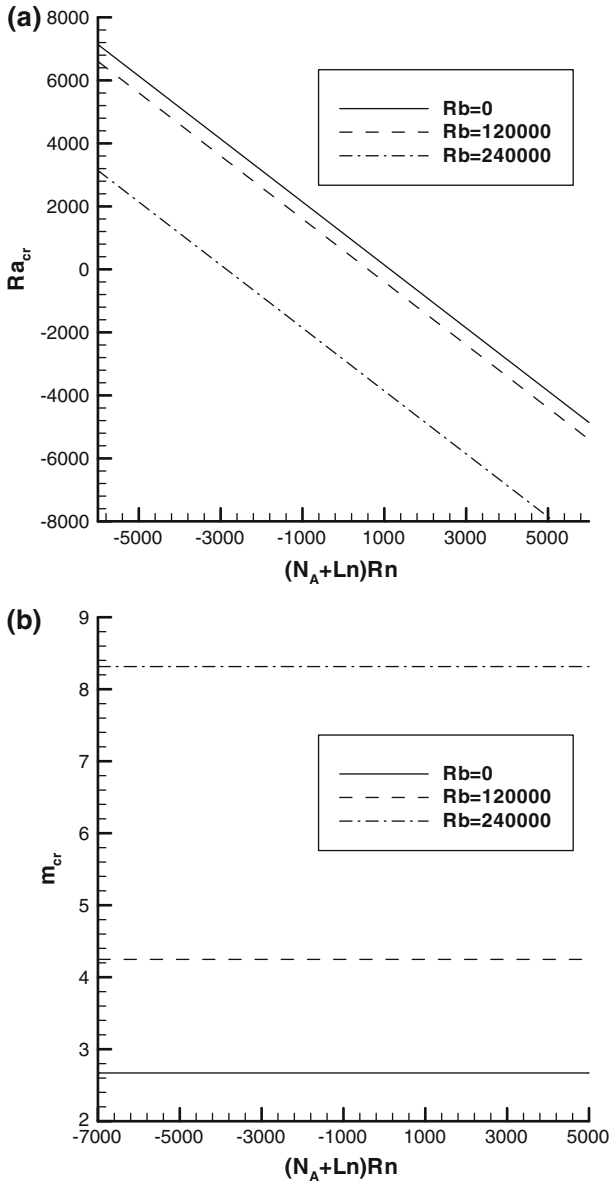

Fig. 6 The same as Fig. 3, but for the case of a rigid lower wall and a stress-free upper wall

Rayleigh–Bérnard problem [31]. The corresponding critical value of $m = 2.670$ is within 0.45% of the exact critical value of $m = 2.682$ [31]. This gives an estimate of the expected accuracy of the one-term Galerkin approximation for this case.

Figure 6 is similar to Fig. 3 but is computed for the rigid-free boundaries, and the same parameter values are utilized. Similar to Fig. 3a, Fig. 6a shows the variation of $\mathrm{Ra}_{\mathrm{cr}}$ versus $(N_A + \mathrm{Ln})\,\mathrm{Rn}$. The effect of microorganisms is still destabilizing, as expected. Notably, the effect of Rb on $\mathrm{Ra}_{\mathrm{cr}}$ is stronger than for the rigid–rigid boundaries. Also, the effect of Rb on the critical wave number displayed in Fig. 6b is stronger than that displayed in Fig. 3b, which indicates that the effect of microorganisms on the critical wave number is more pronounced if the upper boundary is stress free. The trend, however, is the same: the increase in Rb increases the critical value of m.

Figure 7 is similar to Fig. 4 and is computed for the same parameter values; the only difference is that Fig. 7 is for the stress-free upper boundary. The dependencies of $\mathrm{Ra}_{\mathrm{cr}}$ and m_{cr} on ϖ exhibit the same trends as the lines displayed in Fig. 4a and b, respectively, but now the minima in Fig. 7a and the corresponding maxima in Fig. 7b are much sharper and the effect of changing ϖ is stronger.

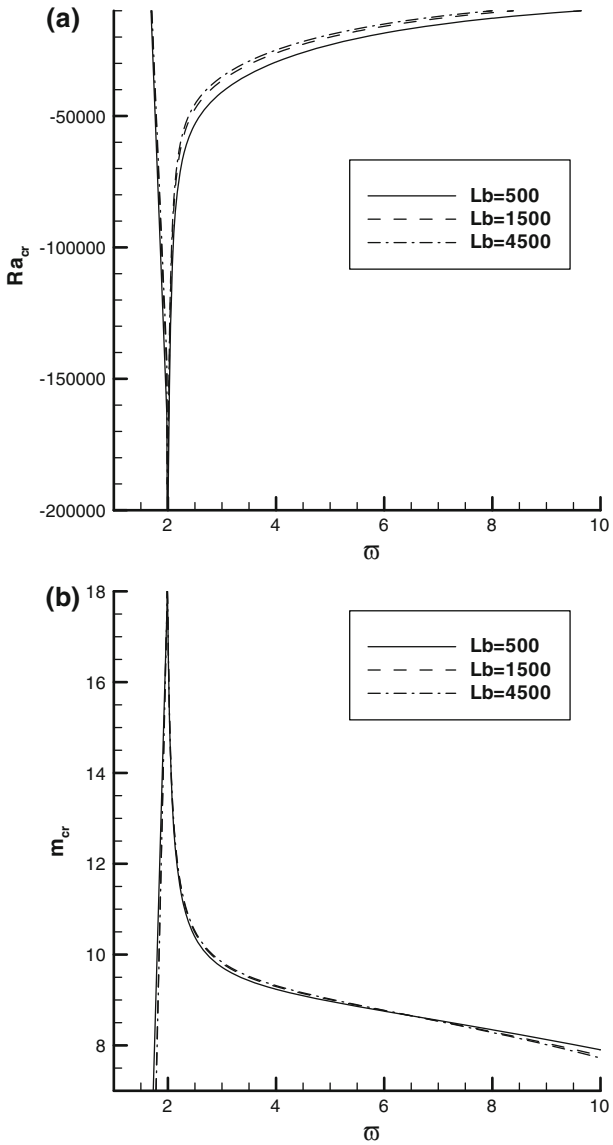

Fig. 7 The same as Fig. 4, but for the case of a rigid lower wall and a stress-free upper wall

Figure 8 is similar to Fig. 5 but is computed for the rigid-free boundaries, and the same parameter values are utilized. Again, the same trends as in Figs. 5a and b are observed, but now the changes of $\mathrm{Ra_{cr}}$ and m_{cr} are stronger, especially with respect to Le.

6 Conclusions

The onset of nanofluid bioconvection is controlled by three agencies. The vertical temperature gradient is destabilizing if heating from the bottom is considered and stabilizing for the case of cooling from the bottom. Nanoparticle concentration is destabilizing if the nanoparticle distribution is top-heavy and stabilizing if it is bottom-heavy. Finally, if the upper surface is open to the atmosphere, the effect of oxytactic microorganisms is destabilizing since they concentrate near the top boundary and contribute toward creating the top-heavy (destabilizing) density stratification.

The case of non-oscillatory instability is investigated. Since the nanoparticle Rayleigh number, Rn, is defined such that positive Rn corresponds to a top-heavy nanoparticle distribution, the increase in Rn produces

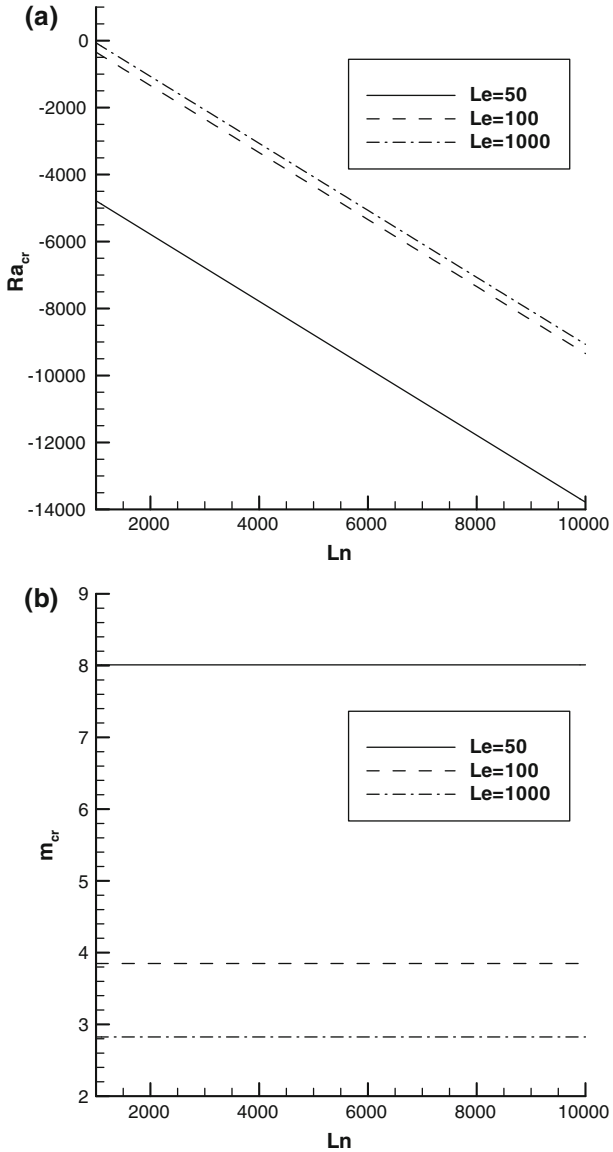

Fig. 8 The same as Fig. 5, but for the case of a rigid lower wall and a stress-free upper wall

the destabilizing effect and reduces the critical value of the thermal Rayleigh number, $\mathrm{Ra_{cr}}$. The increase in the bioconvection Rayleigh number, Rb, produces the destabilizing effect and reduces the critical value of Ra. The latter effect is more pronounced for the stress-free upper boundary. The critical value of the wave number, m_{cr}, is shown to be independent of Rn but depends on Rb; it increases when Rb is increased. This effect is also more pronounced for the stress-free upper wall.

A dependence of $\mathrm{Ra_{cr}}$ on ϖ exhibits a minimum, and a dependence of m_{cr} on ϖ exhibits a maximum at a certain value of ϖ. The minimum and maximum become more pronounced for the rigid-free boundaries. The dependence of $\mathrm{Ra_{cr}}$ on the nanoparticle Lewis number Ln is linear with a negative slope if Rn is positive and with a positive slope if Rn is negative.

Acknowledgments The author gratefully acknowledges critical comments of the anonymous reviewers.

Appendix

The functions F_1 and F_2, defining the non-oscillatory instability boundary for the layer with the rigid–rigid boundaries [given by Eq. (77)] are

$$F_1 = \left\{7A_1\left(10+m^2\right)(14+5\alpha)\left[15I_6\mathrm{Le}\left(I_4+A_1^2I_5m^2\right)+4A_1^2I_1\mathrm{Lb}\left(5+2m^2\right)\varpi\right]\right\} \times\left\{9\mathrm{Lb}\left[I_2\left(5+2m^2\right)-I_4\mathrm{Le}\left(5+2\alpha\right)+m^2\left(I_3\left(5+2m^2\right)-A_1^2I_5\mathrm{Le}\left(5+2\alpha\right)\right)\right]\varpi\right\}^{-1} \quad \text{(A1)}$$

$$F_2 = \frac{28\left(10+m^2\right)\left(504+24m^2+m^4\right)}{27m^2} \quad \text{(A2)}$$

where the integrals $I_1 - I_6$ in Eq. (A1) are functions of Le and ϖ (because A_1, given by Eq. (73), is a function of Le and ϖ and α, given by Eq. (76), is a function of Le and A_1). The expressions for these integrals for the rigid upper-boundary case are given below:

$$I_1 = \int_0^1 \left\{(-1+z)^2z^2\left(1-\frac{1}{2}(-2+z)z\alpha\right)\tan\left[\frac{1}{2}A_1(1-z)\right]\right\}\{1+\cos[A_1(-1+z)]\}^{-1}\,\mathrm{d}z \quad \text{(A3)}$$

$$I_2 = \int_0^1 \left\{\left(1-\frac{1}{2}(-2+z)z\alpha\right)[2\mathrm{Le}\alpha\varpi + A_1^2\mathrm{Le}\left(2-(-2+z)z\alpha\right)\varpi + 2\mathrm{Le}\alpha\varpi\cos[A_1(-1+z)] + 2A_1\mathrm{Le}(-1+z)\alpha\varpi\ \sin[A_1(1-z)]]\right\} \times\{1+\cos[A_1(-1+z)]\}^{-1}\,\mathrm{d}z \quad \text{(A4)}$$

$$I_3 = \int_0^1 \left\{\left(1-\frac{1}{2}(-2+z)z\alpha\right)[\mathrm{Le}\left(2-(-2+z)z\alpha\right)\varpi + \mathrm{Le}\left(2-(-2+z)z\alpha\right)\varpi\cos[A_1(-1+z)]]\right\} \times\{1+\cos[A_1(-1+z)]\}^{-1}\,\mathrm{d}z \quad \text{(A5)}$$

$$I_4 = \int_0^1 \left(1-\frac{1}{2}(-2+z)z\alpha\right)\left[-2A_1^2\varpi + 2A_1^3(-1+z)\varpi\tan\left[\frac{1}{2}A_1(1-z)\right]\right] \times\{1+\cos[A_1(-1+z)]\}^{-1}\,\mathrm{d}z \quad \text{(A6)}$$

$$I_5 = \int_0^1 \left\{(-2+z)z\left(1-\frac{1}{2}(-2+z)z\alpha\right)\varpi\right\}\{1+\cos[A_1(-1+z)]\}^{-1}\,\mathrm{d}z \quad \text{(A7)}$$

$$I_6 = \int_0^1 (-2+z)(-1+z)^2z^3\tan\left[\frac{1}{2}A_1(1-z)\right]\mathrm{d}z \quad \text{(A8)}$$

The functions F_2 and F_3, defining the non-oscillatory instability boundary for the layer with the rigid-free boundaries [given by Eq. (80)] are

$$F_3 = \left\{105A_1\left(10+m^2\right)(126+41\alpha)\left[30\hat{I}_3\hat{I}_5\mathrm{Le}+A_1^2\left(15\hat{I}_4\hat{I}_5\mathrm{Le}m^2+4\hat{I}_1\mathrm{Lb}\left(5+2m^2\right)\varpi\right)\right]\right\} \times\left\{338\mathrm{Lb}\varpi\left(30\hat{I}_2\left(5+2m^2\right)-15\mathrm{Le}\left(2\hat{I}_3+A_1^2\hat{I}_4m^2\right)(5+2\alpha)\right.\right. \left.\left. +\ 4\mathrm{Le}m^2\left(5+2m^2\right)(15+2\alpha\,[5+\alpha])\varpi\right)\right\}^{-1} \quad \text{(A9)}$$

$$F_4 = \frac{28\left(10+m^2\right)\left(4536+432m^2+19m^4\right)}{507m^2} \quad \text{(A10)}$$

where the integrals $\hat{I}_1 - \hat{I}_5$ in Eq. (A9) are functions of Le and ϖ. The expressions for these integrals for the rigid-free upper-boundary case are given below:

$$\hat{I}_1 = \int_0^1 (-1+z)z\left(1+z-2z^2\right)\left(1-\frac{1}{2}(-2+z)z\alpha\right)\sec^2\left[\frac{1}{2}A_1(-1+z)\right]\tan\left[\frac{1}{2}A_1(-1+z)\right]\mathrm{d}z \tag{A11}$$

$$\begin{aligned}\hat{I}_2 = \int_0^1 \left[1-\frac{1}{2}(-2+z)z\alpha\right]\Bigg\{&2\mathrm{Le}\alpha\varpi + \frac{1}{2}A_1^2\mathrm{Le}\left[2-(-2+z)z\alpha\right]\varpi\sec^2\left[\frac{1}{2}A_1(-1+z)\right]\\ &-A_1\mathrm{Le}(-1+z)\alpha\varpi\sec^2\left[\frac{1}{2}A_1(-1+z)\right]\tan\left[\frac{1}{2}A_1(-1+z)\right]\\ &-A_1\mathrm{Le}(-1+z)\alpha\varpi\cos\left[A_1(-1+z)\right]\sec^2\left[\frac{1}{2}A_1(-1+z)\right]\tan\left[\frac{1}{2}A_1(-1+z)\right]\Bigg\}\mathrm{d}z\end{aligned} \tag{A12}$$

$$\begin{aligned}\hat{I}_3 = \int_0^1 \left[1-\frac{1}{2}(-2+z)z\alpha\right]\Big\{&-A_1^2\varpi\sec^2\left[\frac{1}{2}A_1(-1+z)\right] - A_1^3(-1+z)\varpi\sec^2\left[\frac{1}{2}A_1(-1+z)\right]\\ &\times\tan\left[\frac{1}{2}A_1(-1+z)\right]\mathrm{d}z\end{aligned} \tag{A13}$$

$$\hat{I}_4 = \int_0^1 (-2+z)z\left[1-\frac{1}{2}(-2+z)z\alpha\right]\varpi\sec^2\left[\frac{1}{2}A_1(-1+z)\right]\mathrm{d}z \tag{A14}$$

$$\hat{I}_5 = \int_0^1 (-2+z)(-1+z)^2z^2(1+2z)\tan\left[\frac{1}{2}A_1(1-z)\right]\mathrm{d}z \tag{A15}$$

References

1. Do, K.H., Jang, S.P.: Effect of nanofluids on the thermal performance of a flat micro heat pipe with a rectangular grooved wick. Int. J. Heat Mass Transf. **53**, 2183–2192 (2010)
2. Ebrahimi, S., Sabbaghzadeh, J., Lajevardi, M., Hadi, I.: Cooling performance of a microchannel heat sink with nanofluids containing cylindrical nanoparticles (carbon nanotubes). Heat Mass Transf. **46**, 549–553 (2010)
3. Fan, X., Chen, H., Ding, Y., Plucinski, P.K., Lapkin, A.A.: Potential of 'nanofluids' to further intensify microreactors. Green Chem. **10**, 670–677 (2008)
4. Li, H., Liu, S., Dai, Z., Bao, J., Yang, X.: Applications of nanomaterials in electrochemical enzyme biosensors. Sensors **9**, 8547–8561 (2009)
5. Munir, A., Wang, J., Zhou, H.S.: Dynamics of capturing process of multiple magnetic nanoparticles in a flow through microfluidic bioseparation system. IET Nanobiotechnol. **3**, 55–64 (2009)
6. Huh, D., Matthews, B.D., Mammoto, A., Montoya-Zavala, M., Hsin, H.Y., Ingber, D.E.: Reconstituting organ-level lung functions on a chip. Science **328**, 1662–1668 (2010)
7. Sokolov, A., Goldstein, R.E., Feldchtein, F.I., Aranson, I.S.: Enhanced mixing and spatial instability in concentrated bacterial suspensions. Phys. Rev. E **80**, 031903 (2009)
8. Tsai, T., Liou, D., Kuo, L., Chen, P.: Rapid mixing between ferro-nanofluid and water in a semi-active Y-type micromixer. Sens. Actuators A-Phys. **153**, 267–273 (2009)
9. Shitanda, I., Yoshida, Y., Tatsuma, T.: Microimaging of algal bioconvection by scanning electrochemical microscopy. Anal. Chem. **79**, 4237–4240 (2007)
10. Hillesdon, A.J., Pedley, T.J., Kessler, J.O.: The development of concentration gradients in a suspension of chemotactic bacteria. Bull. Math. Biol. **57**, 299–344 (1995)
11. Hillesdon, A.J., Pedley, T.J.: Bioconvection in suspensions of oxytactic bacteria: linear theory. J. Fluid Mech. **324**, 223–259 (1996)
12. Metcalfe, A.M., Pedley, T.J.: Bacterial bioconvection: weakly nonlinear theory for pattern selection. J. Fluid Mech. **370**, 249–270 (1998)
13. Metcalfe, A.M., Pedley, T.J.: Falling plumes in bacterial bioconvection. J. Fluid Mech. **445**, 121–149 (2001)
14. Pedley, T.J.: Instability of uniform micro-organism suspensions revisited. J. Fluid Mech. **647**, 335–359 (2010)
15. Kuznetsov, A.V.: Thermo-bioconvection in a suspension of oxytactic bacteria. Int. Commun. Heat Mass Transf. **32**, 991–999 (2005)

16. Kuznetsov, A.V.: Investigation of the onset of thermo-bioconvection in a suspension of oxytactic microorganisms in a shallow fluid layer heated from below. Theor. Comput. Fluid Dyn. **19**, 287–299 (2005)
17. Kuznetsov, A.V.: The onset of thermo-bioconvection in a shallow fluid saturated porous layer heated from below in a suspension of oxytactic microorganisms. Eur. J. Mech. B-Fluids **25**, 223–233 (2006)
18. Avramenko, A.A., Kuznetsov, A.V.: Bio-thermal convection caused by combined effects of swimming of oxytactic bacteria and inclined temperature gradient in a shallow fluid layer. Int. J. Numer. Methods Heat Fluid Flow **20**, 157–173 (2010)
19. Kuznetsov, A.V., Avramenko, A.A.: Effect of small particles on the stability of bioconvection in a suspension of gyrotactic microorganisms in a layer of finite depth. Int. Commun. Heat Mass Transf. **31**, 1–10 (2004)
20. Geng, P., Kuznetsov, A.V.: Effect of small solid particles on the development of bioconvection plumes. Int. Commun. Heat Mass Transf. **31**, 629–638 (2004)
21. Geng, P., Kuznetsov, A.V.: Settling of bidispersed small solid particles in a dilute suspension containing gyrotactic micro-organisms. Int. J. Eng. Sci. **43**, 992–1010 (2005)
22. Kuznetsov, A.V., Geng, P.: The interaction of bioconvection caused by gyrotactic micro-organisms and settling of small solid particles. Int. J. Numer. Methods Heat Fluid Flow **15**, 328–347 (2005)
23. Geng, P., Kuznetsov, A.V.: Introducing the concept of effective diffusivity to evaluate the effect of bioconvection on small solid particles. Int. J. Transp. Phenom. **7**, 321–338 (2005)
24. Kuznetsov, A.V.: Non-oscillatory and oscillatory nanofluid bio-thermal convection in a horizontal layer of finite depth. Eur. J. Mech. B/Fluids. **30**, 156–165 (2011)
25. Buongiorno, J.: Convective transport in nanofluids. J. Heat Transf.-Trans. ASME **128**, 240–250 (2006)
26. Nield, D.A., Kuznetsov, A.V.: The onset of convection in a horizontal nanofluid layer of finite depth. Eur. J. Mech. B/Fluids. **29**, 217–223 (2010)
27. Nield, D.A., Kuznetsov, A.V.: The effect of local thermal nonequilibrium on the onset of convection in a nanofluid. J. Heat Transf.-Trans. ASME **132**, 052405 (2010)
28. Anoop, K.B., Sundararajan, T., Das, S.K.: Effect of particle size on the convective heat transfer in nanofluid in the developing region. Int. J. Heat Mass Transf. **52**, 2189–2195 (2009)
29. Krishnamurthy, S., Lhattacharya, P., Phelan, P.E., Prasher, R.S.: Enhanced mass transport in nanofluids. Nano Lett. **6**, 419–423 (2006)
30. Finlayson, B.A.: The Method of Weighted Residuals and Variational Principles. Academic Press, New York (1972)
31. Chandrasekhar, S.: Hydrodynamic and Hydromagnetic Stability. Clarendon Press, Oxford (1961)